Polymer 49 (2008) 2717–2727

Contents lists available at ScienceDirect

Polymer

journal homepage: www.elsevier.com/locate/polymer

Rheological studies on the quasi-quiescent crystallization of polypropylene nanocomposites

Tongchen Sun [a,b], Fenghua Chen [a,b], Xia Dong [a,*], Charles C. Han [a,*]

[a] Beijing National Laboratory for Molecular Sciences, Joint Laboratory of Polymer Science and Materials, State Key Laboratory of Polymer Physics and Chemistry, Institute of Chemistry, CAS, Beijing 100190, PR China
[b] Graduate School of the Chinese Academy of Sciences, Beijing 100190, PR China

ARTICLE INFO

Article history:
Received 3 February 2008
Received in revised form 7 April 2008
Accepted 11 April 2008
Available online 1 May 2008

Keywords:
Polypropylene nanocomposite
Rheology
Isothermal crystallization

ABSTRACT

Isothermal crystallization of isotactic polypropylene (iPP)/organic montmorillonite (OMMT) binary nanocomposite and iPP/OMMT/poly(ethylene-*co*-octene) (PEOc) ternary nanocomposites has been investigated by polarized optical microscopy (POM), rheometry and scanning electron microscopy (SEM). At the stage of nucleation the heterogeneous nucleation effect of OMMT was much greater than the concentration fluctuation assisted nucleation effect in the ternary nanocomposite. Besides, PEOc played a role of inhibitor of OMMT nucleation agents at the nucleation stage because many of OMMT layers were distributed around PEOc-rich domains. At stage II of the crystal growth process, the entanglement effect of PEOc greatly affected the rheological response (storage modulus (G') and its growth rate) due to the long side chains of PEOc component. In stage III of the growth process, OMMT layers and the entanglement of PEOc chains limited the motion of polypropylene chains. So the growth rate of G' was slowed down. During the shrinkage and cooling process after isothermal crystallization, some fibril links between the spherulites, consisting of PEOc chains and iPP chains, were formed from the amorphous phases surrounding the spherulites.

1. Introduction

Nanocomposites of polymers with montmorillonite (MMT) have drawn increasing attention in recent years because of their significant improvement of physical and/or chemical properties over the matrix polymers [1–4]. The effect of clay on these properties has been extensively investigated. The addition of just a few percent by weight of clay can result in significant improvement in mechanical properties. Many studies have been systematically carried out focusing on the relationship between the micro-structure and the meso- or macroscopic properties [5–8], especially for the semi-crystalline polymers, such as polypropylene, polyamide and polyester, where the crystalline behaviors play an essential role in determining the ultimate properties of these nanocomposites.

Polypropylene/clay nanocomposite is of great interest in the field of nanocomposites because of its industrial importance. Many studies have been conducted on neat polypropylene with or without shear field [9–27]. The crystallization and the morphology of iPP were investigated by different measurements, such as differential scanning calorimetry (DSC), optical microscopy, rheology, and light or X-ray scattering and a fruitful amount of results have been obtained. The complicated nature and mechanism of neat polymer crystallization are fundamentally understood. The crystallization kinetics of neat polypropylene is determined by the nucleation and spherulite growth rate. The addition of nano-clay greatly influenced the crystallization behavior of iPP. Effects of nano-clay layers were considered in two aspects: (i) nano-clay layer could be an effective heterogeneous nucleation agent [28–31] that decreased the interfacial free energy per unit area perpendicular to macromolecular chains in the nanocomposites. This could enhance the nucleation rate and consequently the increased number of nuclei, and decreased the size of spherulite; (ii) a physical hindrance was created by the nano-clay layers to the motion of polymer chains, which limited the crystal growth in the polymer matrix [32,33], resulting in a decrease of the degree of crystallinity and the degree of perfection of the spherulite.

Although polypropylene/clay binary nanocomposite shows a great improvement in properties compared with the neat polypropylene, there are still some disadvantages in this composite. The major deficiency is a low impact resistance, particularly at low temperatures. Therefore, a third component, usually an elastomer, was introduced to modify this system [34–41], which greatly improved the impact strength and elongation at break of neat polypropylene and PP/clay composites as well. The toughening effect of elastomer has been examined for semicrystalline polymer/elastomer binary system before [42–46]. Since the macroscopic

* Corresponding authors. Tel.: +86 10 82618089; fax: +86 10 62521519.
E-mail addresses: xiadong@iccas.ac.cn (X. Dong), c.c.han@iccas.ac.cn (C.C. Han).

0032-3861/$ – see front matter © 2008 Elsevier Ltd. All rights reserved.
doi:10.1016/j.polymer.2008.04.021

properties are determined by the micro- or meso-scale structure, the formation processes of these structures which include the phase separation and crystallization of these binary systems under quiescent and shear conditions have become the center of attention for researchers working in this area [47–57]. For example, in the coupling process of phase separation and crystallization under quiescent condition, the effect of concentration fluctuation assisted nucleation can greatly speed up the crystallization of these systems at the early stage of phase separation, which have been reported in poly(ethylene-*co*-hexene) (PEH)/poly(ethylene-*co*-butene) (PEB) and PEH/poly(ethylene-*co*-octene) (PEOc) binary blend [50–55].

Although some great achievements have been obtained for iPP/OMMT composite and iPP/elastomer blends, there are few details available about the iPP/OMMT/PEOc ternary composite. Much important information has not been reported and questions not answered, such as the crystal structure of this composite, the heterogeneous nucleation effect of OMMT layers in the ternary composite, and the final morphology of these composites.

In this paper, we will report on the study of the quiescent isothermal crystallization of iPP/OMMT binary and iPP/OMMT/PEOc ternary composites by rheometry, and also the characteristic crystal morphology, which relates to the storage modulus of bulk material during isothermal crystallization process, obtained through POM. Based on the POM and rheological measurement results of these two kinds of composite, the effect of clay layers and PEOc at different stages of isothermal crystallization was obtained. With the final morphology observed by SEM, a schematic model was proposed to explain the isothermal crystallization process of these materials.

2. Experimental

2.1. Materials and preparation

iPP (trade marked as T30s, Yan Shan Petroleum China) and PEOc (Engage 8150, Dupont Dow Elastomer) with the content of octene 30.6 wt% [46] were used as the matrix materials. Sodium montmorillonite with a cation exchange capacity of 68.8 mmol/100 g (RenShou, Sichuan, China) was organically modified through ion-exchanged reaction with dioctadecyl dimethylammonium bromide. Maleic anhydride (MA) modified polypropylene (PPgMA) with the content of MA 0.9 wt% was used as the compatibilizer, which was purchased from Chen Guang Co. (Sichuan, China). The characteristic parameters of these samples are listed in Table 1. Samples were prepared in the same way as the previous work [41]. The blend of iPP/PPgMA with the compositional ratio of 90/10 by weight was used as the base resin. The clay layers were intercalated and partially exfoliated and well dispersed in the polymer matrix. The prepared samples were marked as PPCN*x* for iPP/PPgMA/OMMT and PPCN*x*OE*y* for iPP/PPgMA/OMMT/PEOc nanocomposites (*x* and *y* stood for the contents of OMMT and PEOc, respectively. The unit was defined as phr (part per hundred parts of iPP/PPgMA)).

2.2. Measurements and characterization

2.2.1. Rheological measurement

All rheological experiments were conducted with an Advanced Rheometric Expansion System (ARES, Rheometric Scientific, NJ) which was a strain-controlled rheometer with a cone-plate fixture (25 mm diameter, 0.1 radian cone angle). Disk samples were prepared by compression molding with 1.2 mm in thickness and 25 mm in diameter. The sample was put on the lower plate at 200 °C and held for 5 min to eliminate the mechanical and heat history. Then slowly lower the upper plate to get the center gap 48 μm. Held at 200 °C for another 10 min, the sample was then cooled to 140 °C quickly. Once the temperature reached 140 °C, dynamic time sweep experiment was immediately carried out at a frequency of 1 rad/s and a strain of 1%. All of the measurements were carried out under a nitrogen atmosphere to avoid oxidative degradation of the specimens.

Table 1
The characteristic parameters of materials used in experiments

Sample	M_w (g/mol)	M_w/M_n
iPP	4.0×10^5	4.7
PPgMA	2.1×10^5	3.2
PEOc	1.4×10^5	2.2

2.2.2. Polarized optical microscopy

A small amount of material was sandwiched between a glass slide and a cover glass with a polyimide spacer (50 μm thickness). The sample was put on a hot stage (Linkam LTS350), and annealed at 200 °C for 10 min to eliminate the mechanical and thermal history. Then the temperature was quickly decreased to 140 °C and the isothermal crystallization process was observed with a polarized optical microscope (Olympus BX51).

2.2.3. Scanning electron microscopy

After POM experiment, the sample was cryogenically fractured into four parts in liquid nitrogen, and sample was peeled off from the cover glass. Then one part of the sample was directly observed under a scanning electron microscope. Some selected samples were etched by xylene at ambient temperature for 5 days to dissolve the PEOc-rich phase. And some other samples were immersed in a solution of 0.25 wt%/v potassium permanganate in a 3:2:5 (volume ratio) mixture of orthophosphoric and sulphuric acids and water for 5 min to etch out the amorphous phases. All of the samples were coated with platinum prior to the examination with a scanning electron microscope (JEOL JSM 6700F).

3. Results and discussion

It was believed that dynamic time sweep with small frequency and strain had no effect on the crystal structure development of polymer [17–24,27]. So it was employed to monitor the isothermal crystallization process of polypropylene composites in this study. Fig. 1 shows the overall process of isothermal crystallization at 140 °C detected by the rheometer and the corresponding polarized optical micrographs of sample PPCN0.5. The storage modulus (G') of bulk material between the plates developed with the crystallizing time (t). Initially, the size of spherulites was very small and they were far away from each other. They did not have effective interactions with each other through the entangled molecules between the spherulites. Correspondingly, G' did not change much before $t = 45$ min. With the growth of spherulites, they started to have effective interactions with each other through the entangled polymer network between the spherulites and a physical gel was formed as Winter proposed [17–21]. At this time, G' began to increase. The rate of increase became faster when the spherulites came into contact with each other around 70 min for PPCN0.5. When the spherulites impinged into each other like the structure at $t = 98$ min, the increase rate of storage modulus slowed down. Finally, G' turned to be constant, and at this moment the crystallization was almost complete. The whole process of crystallization can be divided into two stages: nucleation and crystal growth. The nucleation process cannot be observed directly by POM, but the number of nuclei can be clearly confirmed by counting the number of spherulite in Fig. 1(c). According to the intensity of interaction between spherulites, the crystal growth process, with the rheological curve in Fig. 1(a), can be divided into three stages: stage I (Fig. 1(c)) where G' did not change much, stage II (Fig. 1(d)) where G' increased greatly and the growth rate of G' was also increased

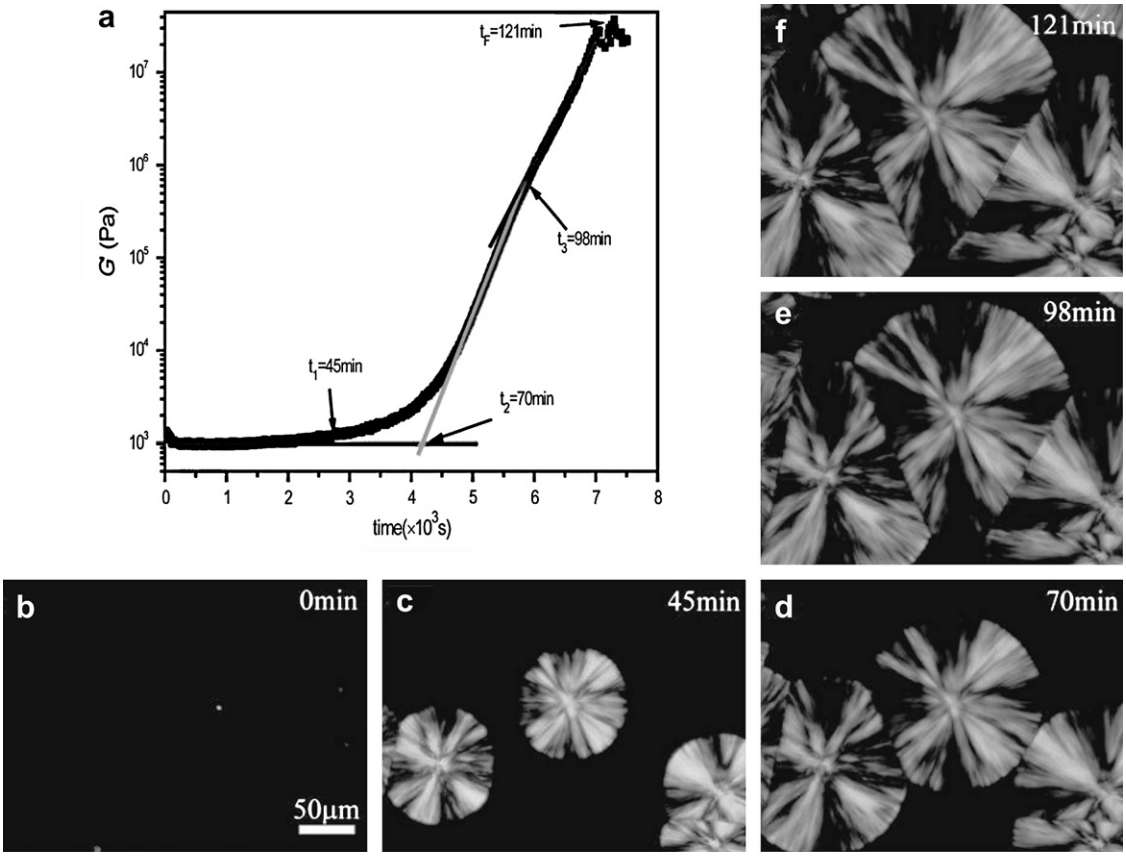

Fig. 1. Storage modulus of PPCN0.5 as a function of crystallizing time and the corresponding polarized optical micrographs during isothermal crystallization process at 140 °C.

and stage III (Fig. 1(e)) where the growth rate of G' was slowed down slightly. And the effect of OMMT and PEOc on crystallization at different stages of isothermal crystallization will be discussed in detail later.

3.1. The effect of OMMT on crystallization behaviors of iPP/OMMT binary nanocomposites

Fig. 2(a) shows the storage modulus vs. crystallizing time of iPP/OMMT binary composites with different OMMT contents. With the increase of clay content the time when G' turned upward became shorter. The corresponding crystal structures of these five composites at $t = 35$ min are shown in Fig. 3. The number of spherulites increased with the increase of clay content, which meant that the number of nuclei increased with the increase of clay content at the nucleation stage. Therefore the clay layers must have played a great role in the promotion of nucleation and consequently in the crystallization of iPP/OMMT nanocomposites. Assuming that growth rate of spherulites was roughly the same, more nuclei would result in more spherulites, and consequently would result in more contact

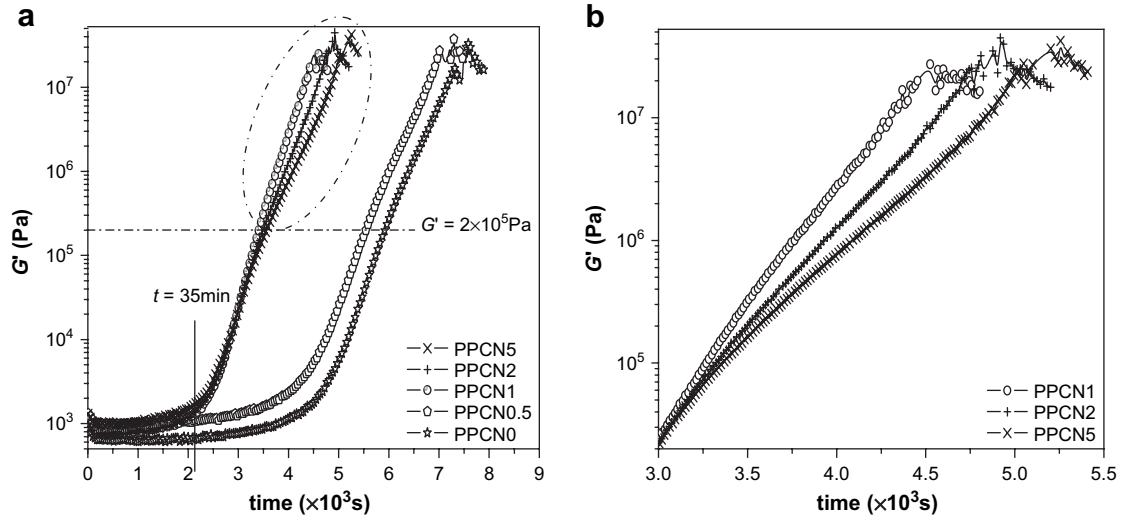

Fig. 2. Time dependence of (a) storage moduli of iPP/OMMT binary nanocomposite samples and (b) storage moduli of PPCN1, PPCN2 and PPCN5 samples after $t = t_{G'=2\times10^5\ \mathrm{Pa}}$, magnification of the circled part in panel (a).

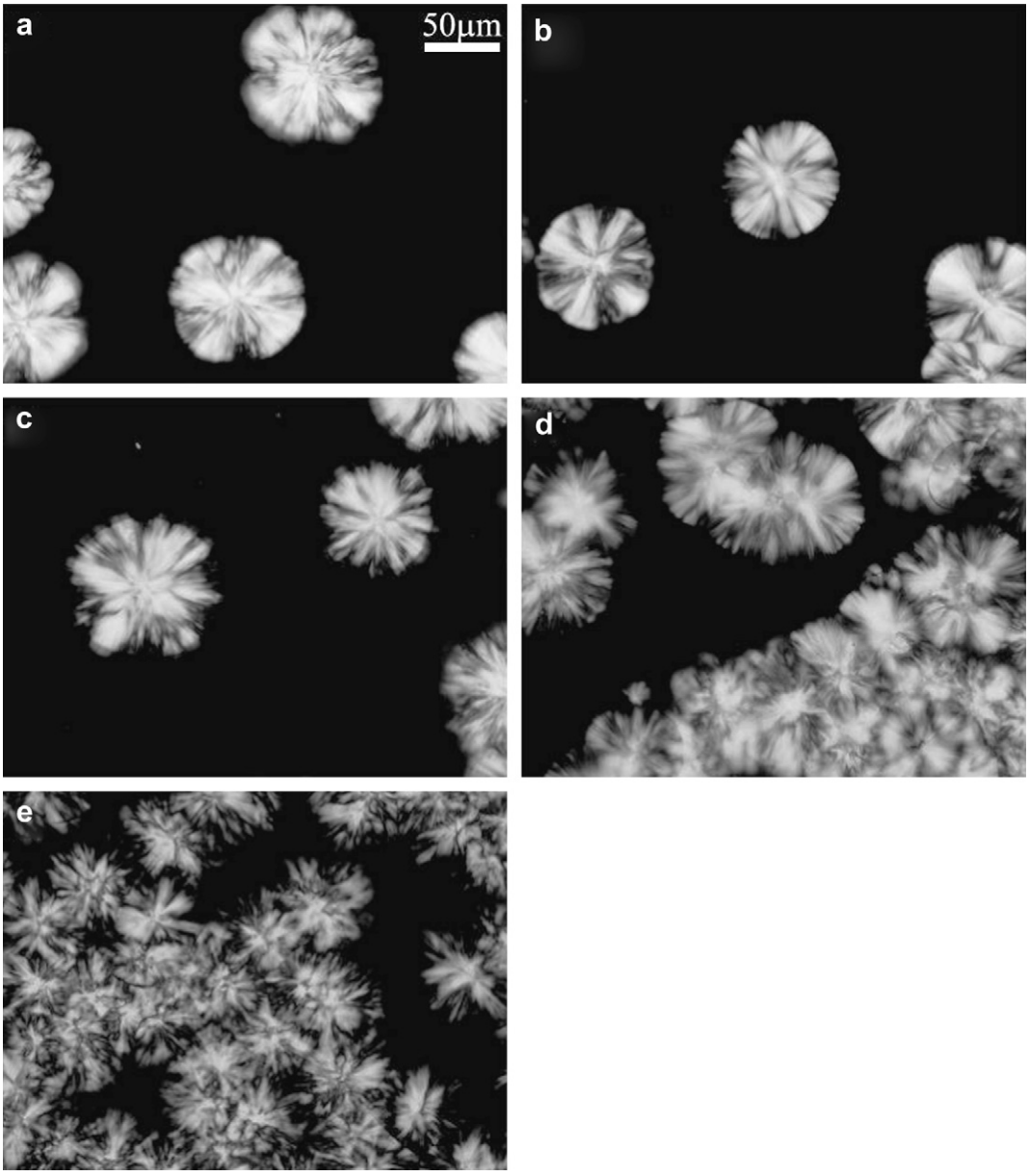

Fig. 3. POM images of (a) PPCN0, (b) PPCN0.5, (c) PPCN1, (d) PPCN2 and (e) PPCN5 at $t = 35$ min during isothermal crystallization process at 140 °C.

or stronger interactions between the crystals in the same volume. So the storage moduli of iPP/OMMT bulk materials with higher OMMT content changed upward earlier. However, the nucleation kinetics of clay layers could not be clearly analyzed from the rheological curves when the clay content was about 1–5 phr. Since the clay layers acting as heterogeneous nucleation agents resulted in many spherulites in these high OMMT content samples, the formed spherulites could affect the storage modulus of the bulk material, especially when these spherulites started to interact with each other at stage II of the growth process.

For PPCN1, PPCN2 and PPCN5, G' vs. t curves after $t = t_{G'=2\times10^5\ \mathrm{Pa}}$ are shown in Fig. 2(b). When clay content was above 1 phr, the growth rate of G' at this stage became slower with the increase of clay content. The corresponding crystal structures of these five materials at $t = t_{G'=2\times10^5\ \mathrm{Pa}}$ are shown in Fig. 4. Spherulites began to impinge into each other and almost huddled together in all of these five samples. After this time, the growth rate of spherulite and the corresponding growth rate of G' were slowed down slightly, and the process proceeded into stage III of the growth process. The slow down of spherulite growth rate was probably caused by the following reasons:

(i) The entanglement of polymer chains with clay layers limited the motion of polymer chains which would be re-arranged into the crystal in the bulk. Especially when the clay content reached a certain value, a three-dimensional network of the clay layers might be formed and the iPP chains might entangle together with the clay network. This entangled meso-scale network structure could play a role of hindrance in the motion of polypropylene chains. The hindrance effect became stronger with the increase of clay content. So the motion and rearrangement of polypropylene chains became more difficult and the growth rate of spherulite was decreased with the increase of OMMT content.

(ii) After $t = t_{G'=2\times10^5\ \mathrm{Pa}}$, the spherulites were huddled together. They impinged into each other and the interface area between the spherulites and the amorphous regions was diminished. With the crystallizing time going on, the content of iPP chains

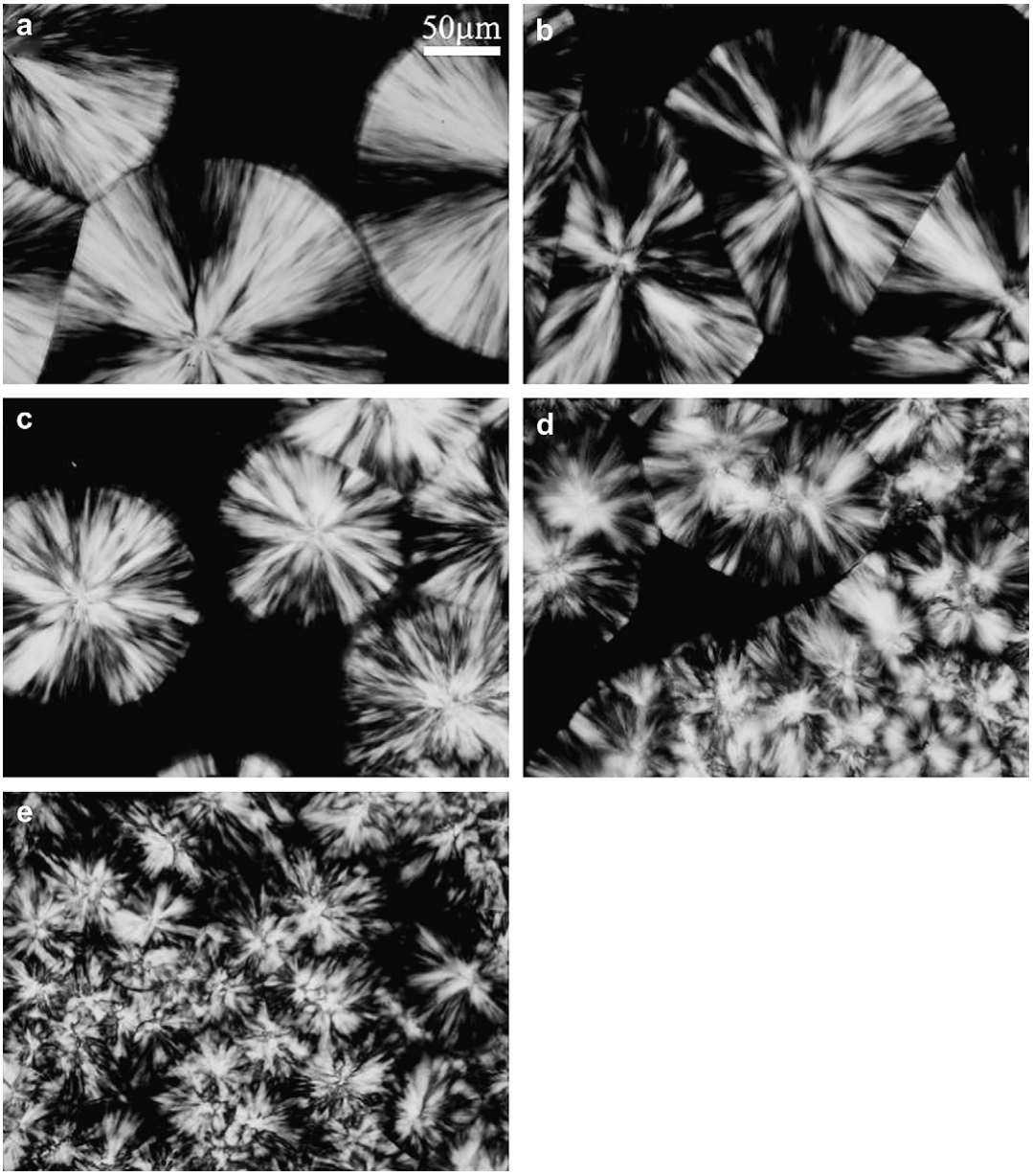

Fig. 4. POM images of (a) PPCN0, (b) PPCN0.5, (c) PPCN1, (d) PPCN2 and (e) PPCN5 when $G' = 2 \times 10^5$ Pa during isothermal crystallization process at 140 °C.

which were transported from amorphous phase to crystal phase was decreased in the same time so that the growth rate of spherulites was slowed down and the corresponding increase rate of storage modulus was slowed down too.

(iii) There were fewer polypropylene chains left in the amorphous phases of the materials. So the re-arranging motion of polypropylene chains from amorphous phase to crystalline phase became more and more difficult and the growth rate slowed down.

3.2. The effect of OMMT and PEOc on the crystallization behaviors of iPP/OMMT/PEOc ternary nanocomposites

Fig. 5 shows the comparison between the binary nanocomposites and ternary nanocomposites with the same OMMT content (PPCN0 vs. PPCN0OE15 and PPCN2 vs. PPCN2OE15). The storage modulus of PPCN0OE15 changed upward and reached the plateau earlier than that of PPCN0. The same thing happened to PPCN2OE15 and PPCN2, although the difference between PPCN2OE15 and PPCN2 was smaller than that between PPCN0OE15 and PPCN0. This might be explained by the following two arguments:

(i) Based on the previous study on PEH/PEB and PEH/PEOc binary systems [50–55], compositional fluctuation coming from liquid–liquid phase separation could assist the nuclei formation in the crystallization process. The liquid–liquid phase separation process in the iPP/OMMT/PEOc ternary nanocomposites could certainly increase the rate of nucleation for the iPP crystallization. This coupled process could be also affirmed by the nucleation number difference between PPCN0OE15 and PPCN0 as shown in Fig. 6(a) and (b) which showed the crystal structures of these four nanocomposite samples at the time when $G' = 2 \times 10^5$ Pa.

(ii) With the progress of phase separation of the ternary nanocomposites, some PEOc-rich domains were formed, which acted as viscoelastic components in samples, when rheological

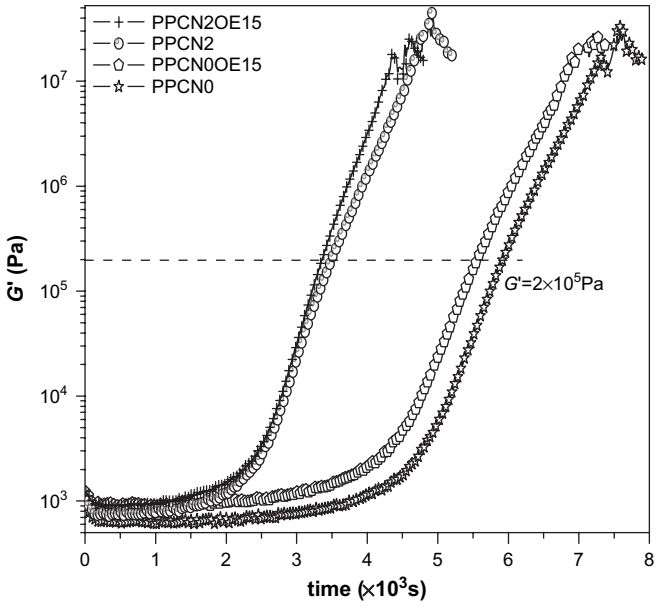

Fig. 5. Time dependence of storage moduli of PPCN0, PPCN0OE15, PPCN2 and PPCN2OE15 during isothermal crystallization process at 140 °C.

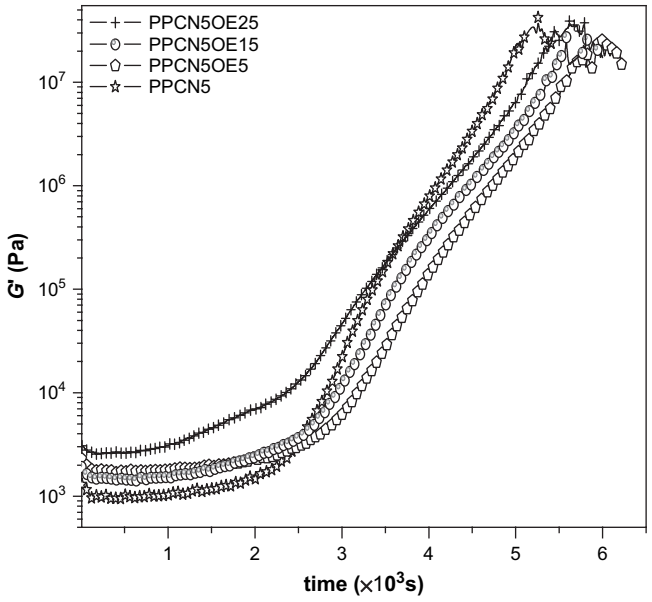

Fig. 7. Storage moduli of PPCN5OE*y* as a function of isothermal crystallizing time at 140 °C.

experiments were conducted. These viscoelastic domains interconnected with the rigid spherulites could greatly increase the storage modulus, G', during the rheological measurements. So the rheological response of the ternary nanocomposite sample was ahead of that of binary one.

In Fig. 6(c) and (d), the amount of spherulites of PPCN2OE15 was smaller than that of PPCN2. That meant that the nucleation effect of clay layers was actually inhibited by PEOc at the stage of nucleation, which was in accord with the previous work [41]. Many of the clay layers were localized close to or inside the PEOc-rich domains. Therefore, this part of clay layers could not act as nucleation agents for the iPP crystallization. Besides, in Fig. 6(b) and (d), the spherulites' (nucleation) number of PPCN2OE15 was larger than that of PPCN0OE15, which implied that the heterogeneous nucleation effect of clay layers was much greater than the effect of concentration

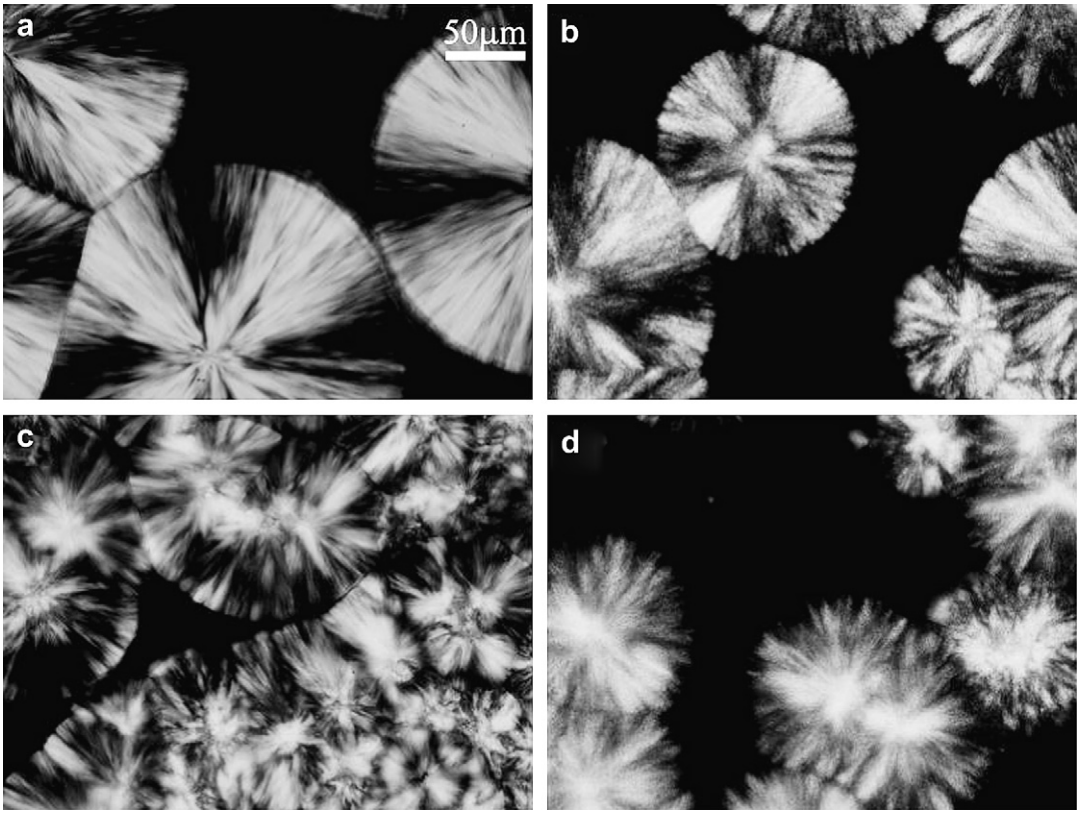

Fig. 6. POM images of (a) PPCN0, (b) PPCN0OE15, (c) PPCN2 and (d) PPCN2OE15 when $G' = 2 \times 10^5$ Pa during isothermal crystallization process at 140 °C.

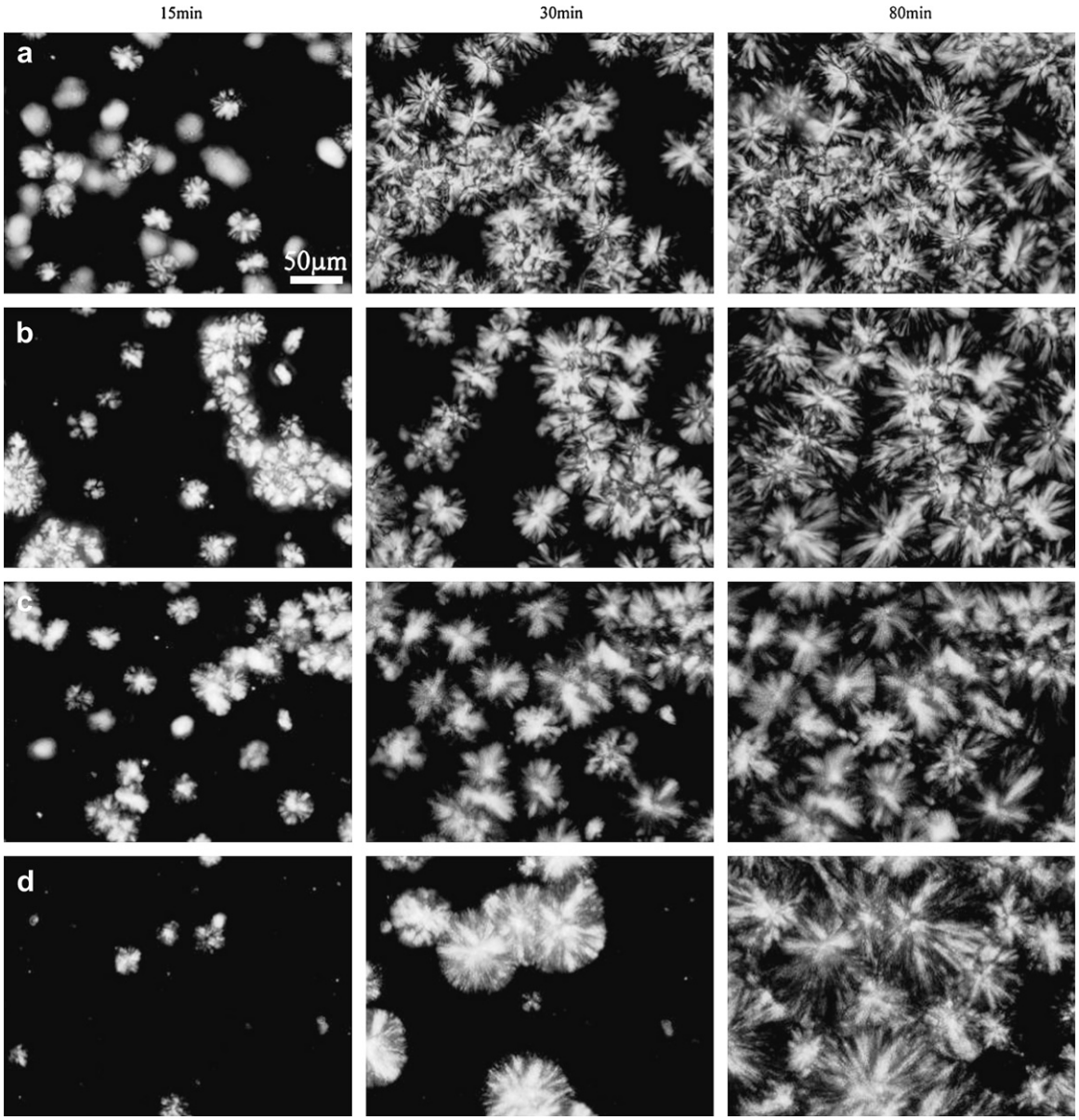

Fig. 8. POM images of (a) PPCN5, (b) PPCN5OE5, (c) PPCN5OE15 and (d) PPCN5OE25 during isothermal crystallization at 140 °C at $t = 15$ min, 30 min and 80 min.

fluctuation assisted nucleation. So the crystallization time difference between PPCN2 and PPCN2OE15 was smaller compared with that between PPCN0 and PPCN0OE15 as indicated in Fig. 5.

Fig. 7 shows the time dependence of G' of PPCN5OE*y* during isothermal crystallization at 140 °C. The initial G' of bulk material was generally increased with the addition of PEOc. With the increase of PEOc content, the increase of G' was delayed for PPCN5OE5 and PPCN5OE15. And the overall growth rate of G' of these three ternary nanocomposite samples was slower than that of PPCN5. It might be caused by the inhibition effect of PEOc-rich domains, which was mentioned earlier in the explanation of the crystallization difference between PPCN2 and PPCN2OE15. This could be confirmed by Fig. 8 which showed the crystal structures of these four samples. Comparing the POM images at the same crystallizing time as shown in Fig. 8, it was clear that the spherulite number was decreased obviously with the increase of PEOc content, which was in accord with the difference between Fig. 6(c) and (d). This provided another evidence to prove our speculation: compared with the effect of concentration fluctuation assisted nucleation, the heterogeneous nucleation effect of clay layers was the dominant one in the isothermal crystallization process of iPP/OMMT/PEOc ternary composites. However, the addition of PEOc would actually hinder the nucleation by OMMT.

Comparing the time dependence of G' curves of these three ternary composites, we could find that the upward-change of G' became earlier with the increase of PEOc content. And the storage modulus of PPCN5OE25 changed upward the earliest, although there was the smallest amount of spherulites of this sample at the same crystallizing time as shown in Fig. 8. This could be explained by the following facts: (i) with the increase of PEOc content, the size and relative volume of phase separated PEOc-rich domains became larger at the late stage of phase separation. The rigid spherulite domains were interconnected through the highly viscoelastic phase separated PEOc-rich domains. This network could greatly enhance the storage modulus. (ii) With the increase of PEOc content, the effect of fluctuation assisted crystallization became greater, although this was very important when OMMT content was zero, and became a minor effect when OMMT was present. However, the crystal spherulites could interact with each other and formed a network earlier through the connection of PEOc domains,

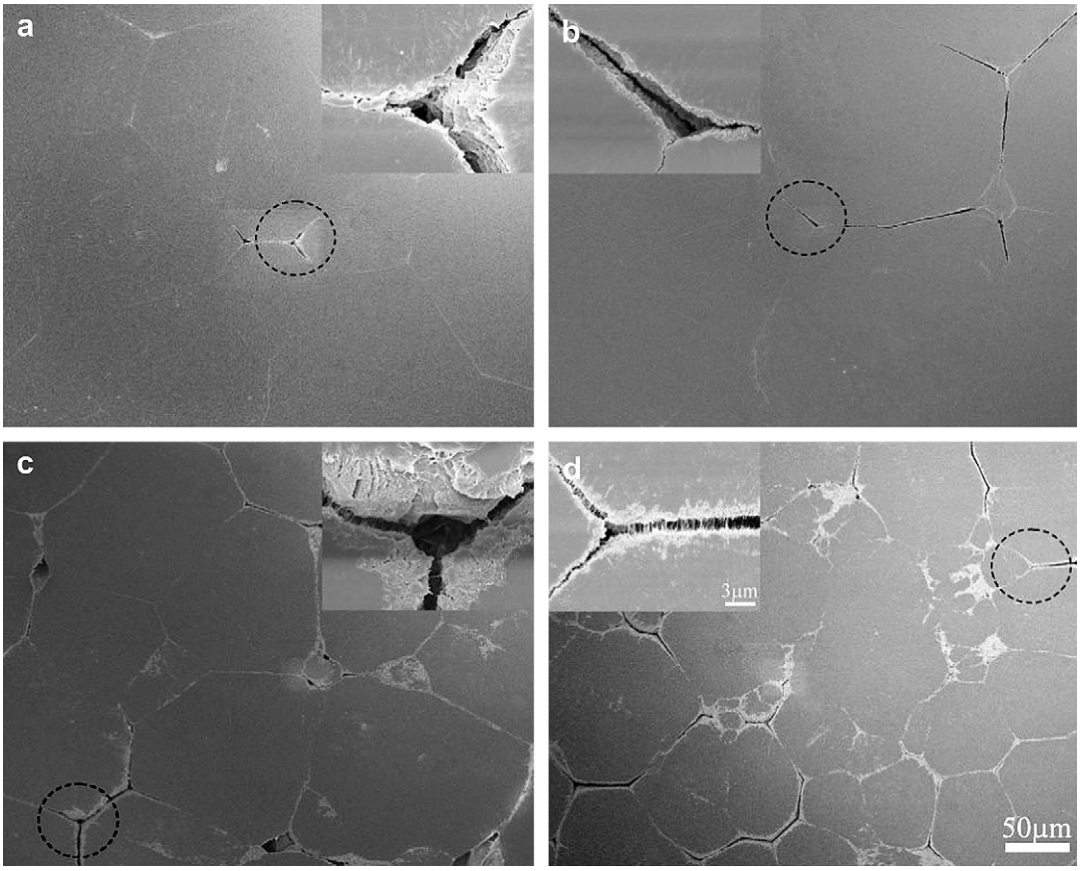

Fig. 9. SEM images of the final morphologies of (a) PPCN0, (b) PPCN0.5, (c) PPCN2 and (d) PPCN5. The inset is the magnification of the marked region, respectively.

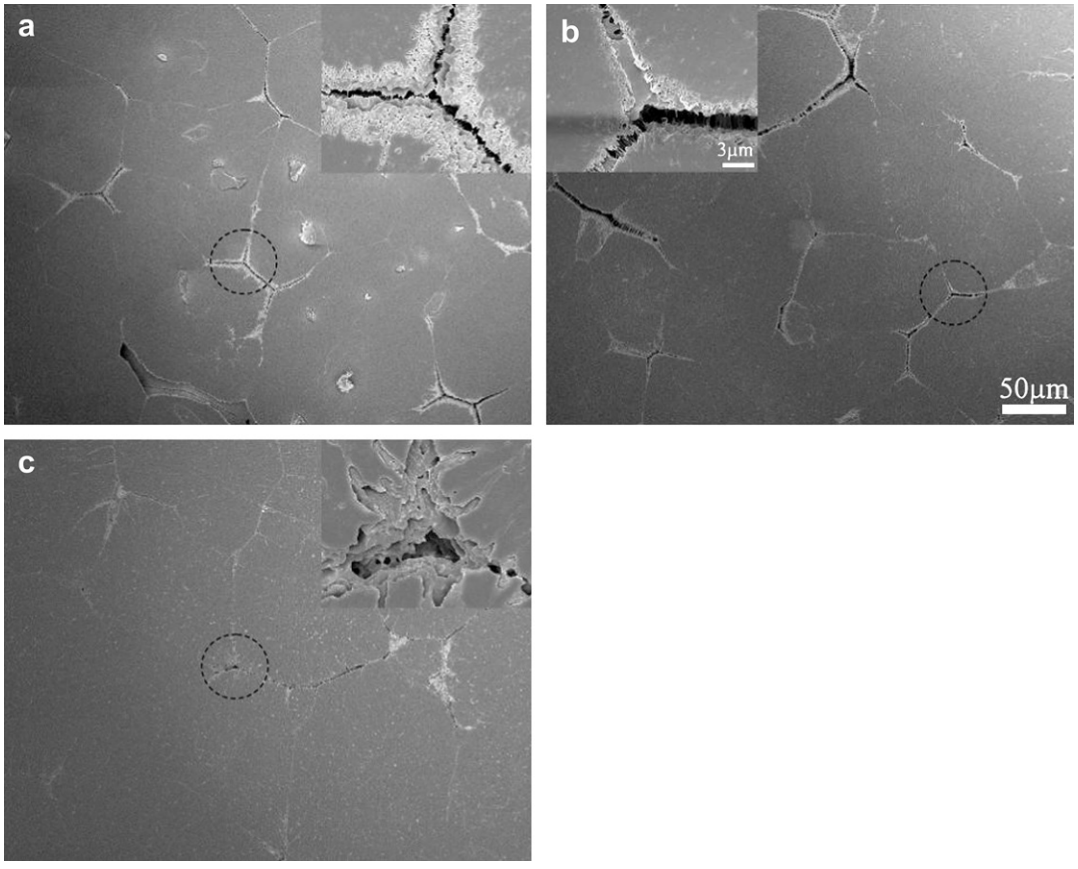

Fig. 10. SEM images of the final morphologies of (a) PPCN5OE5, (b) PPCN5OE15 and (c) PPCN5OE25. The inset is the magnification of the marked region, respectively.

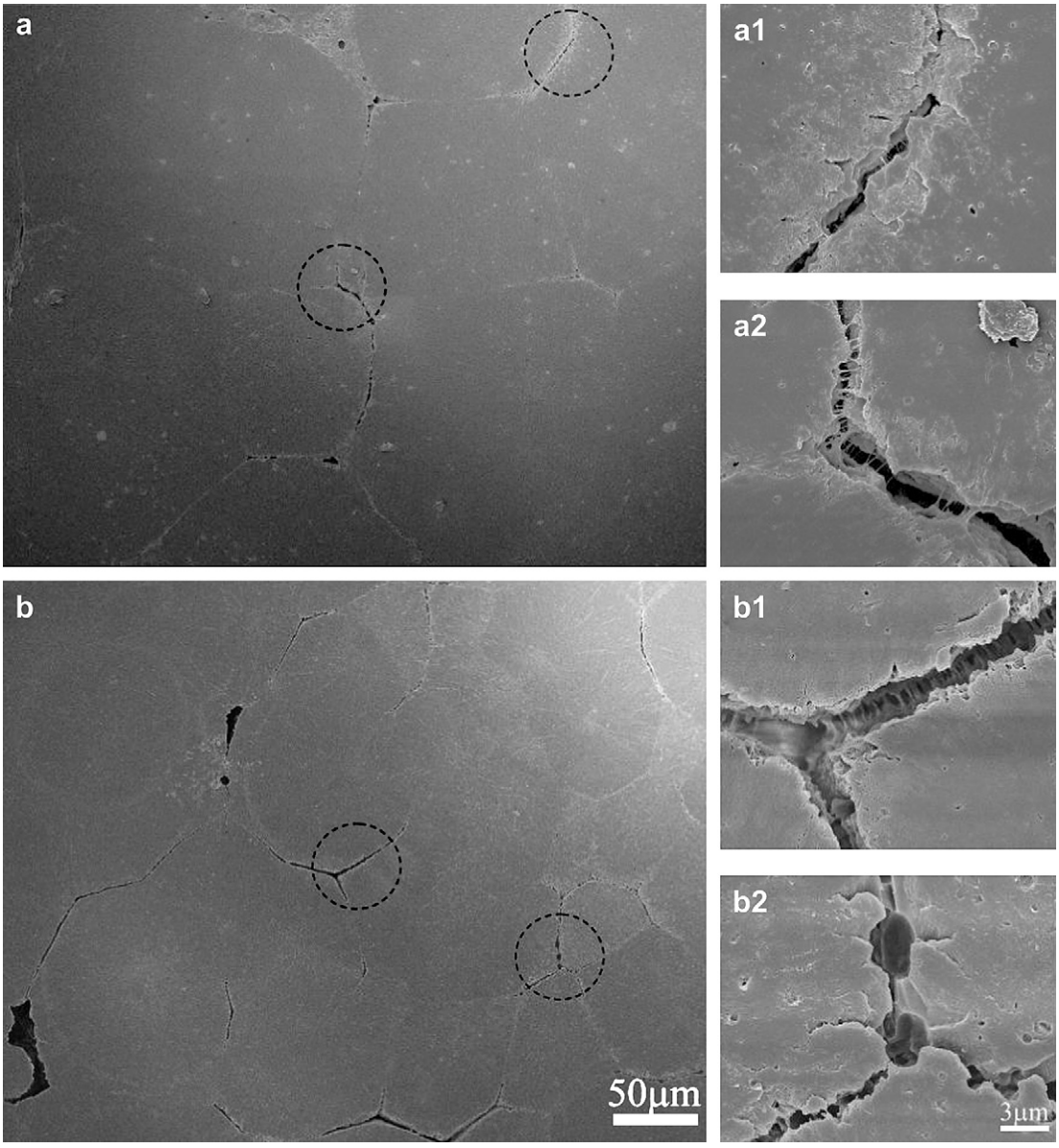

Fig. 11. SEM images of PPCN5OE15 samples: (a) etched by xylene at room temperature for 5 days and (b) etched by the acid solution at room temperature for 5 min. The right panels are the magnifications of the marked regions, respectively.

therefore, in rheological response, the storage modulus changed upward earlier with the increase of PEOc content.

3.3. The final crystallization morphologies of these composites

After crystallization experiments were completed at 140 °C, samples which had been used in POM observation were quickly quenched to room temperature. These samples were peeled off from the cover glass after liquid nitrogen cooled and examined by SEM to obtain the final morphology. Fig. 9 shows the SEM images of the structures of four iPP/OMMT binary composite samples without being etched after crystallization was complete. The inset in each panel is a magnified image of the area marked with a circle. It was clear that the size of spherulites was decreased with the increase of clay content. This result was consistent with that obtained from POM observation, i.e., with the increase of OMMT content, the heterogeneous nucleation effect was enhanced and the number of nuclei was increased. So the crystal size and perfection were both decreased. From these insets we could find that there were some links (whisker-like structures) formed between the spherulites. And the amount of these interspherulite phases was increasing with the increase of OMMT content. Similar observation had been reported in the thin film (about 100 nm or less in thickness) of polyethylene (PE)/*n*-$C_{32}H_{66}$ system by Keith et al. [58–61]. In their case, the formation of links was strongly influenced by molecular weight of PE and isothermal crystallizing temperature. High molecular weight of PE and low crystallizing temperature were beneficial for the formation of intercrystalline links. They suggested that these links were formed from the molecules which were entangled with neighboring molecules during the crystallizing process. Although many of the links showed no sharp reflections at all when electron diffraction experiment was conducted, they proposed that the links might be extended-chain single crystals. In order to confirm the characteristics of the links in our case, another series of experiments were designed with the samples of PPCN5OE*y*.

Fig. 10 shows the SEM micrographs of PPCN5OE5, PPCN5OE15 and PPCN5OE25 without being etched. The size of spherulites was

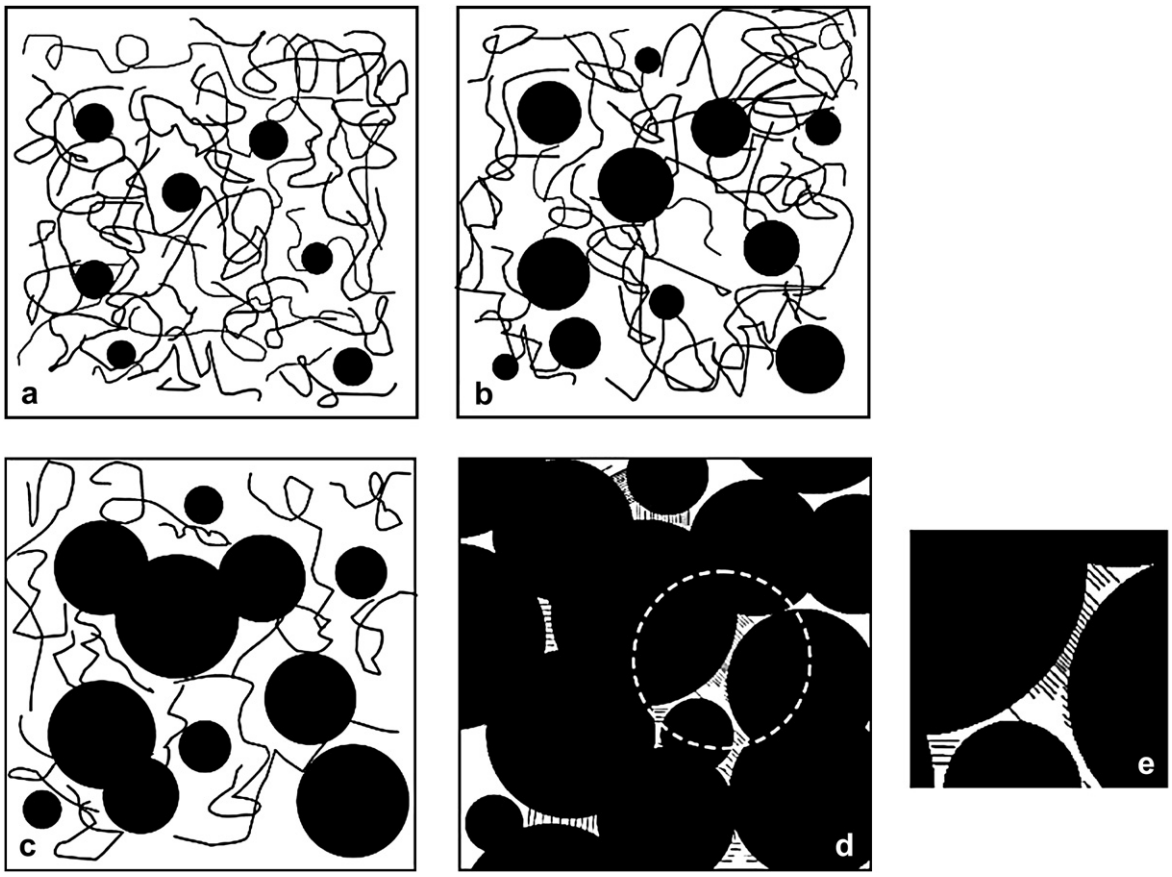

Fig. 12. A schematic model of the isothermal crystallization process: (a) stage I, (b) stage II, (c) stage III of the crystal growth process and (d) the final morphology of the sample with the circled part magnified as (e). (The lines shown in (d) and (e) represent the links (whiskers and film) between the spherulites.)

increased with the increase of PEOc content, which was in accord with the POM results and our speculation in Section 3.2. The gap between the spherulites became thinner with the increase of PEOc content. Even in PPCN5OE25 there were only very few cleavage between the spherulites. During the crystallizing process, the amorphous phases were squeezed out of the crystalline region to the interspaces between spherulites. With the increase of PEOc content, the interspaces between the spherulites were even filled with the increased amorphous phase (mainly PEOc phase) in PPCN5OE25. From the insets it was clearly observed that there were links (including whisker and film) formed between the spherulites. Based on these experimental results, we would like to speculate that these structures were formed due to the stretching of the amorphous phases between the spherulites, which were entangled with the neighboring spherulites, during the cooling and shrinkage process after crystallization. The entangled polymer chains between the spherulites were stretched and extended to form these whisker and film like structures. These links were formed from the amorphous phases in the much thicker samples than PE/*n*-$C_{32}H_{66}$ film which was mentioned in Refs. [57–60]. Then the next question was about the properties of these interphase structures: crystalline or amorphous?

Fig. 11 shows the structures of PPCN5OE15 etched by (a) xylene and (b) the acid solution separately. The pictures in the right column are corresponding to the marked areas in the left panels. After the sample was etched by xylene, the amount of whisker-like structures was decreased but there were still some existing. This indicated that these whiskers were consisted of not only PEOc chains but also polypropylene chains. After the sample was immersed in the acid solution for 5 min, not only the whiskers on the surface were etched out as shown in Fig. 11(b1), but also some amorphous phases disappeared as shown in Fig. 11(b2). This implied that the intercrystalline phases were amorphous and consisted of iPP and PEOc components.

According to the rheological curve of bulk material and POM and SEM examinations, the whole crystallization process could be divided into three stages, i.e., nucleation, crystal growth and shrinkage. As for nucleation process which could be implied by the POM indirectly, it was greatly affected by OMMT layers and PEOc component which had been clearly explained before. The crystal morphology and corresponding storage modulus development of the composite could be obtained directly from the POM and the rheometric measurements during the growth process. The schematic model of the crystal growth process was proposed as shown in Fig. 12, where three stages were depicted as (a) stage I, (b) stage II and (c) stage III, according to the interaction between spherulites and the rheological curves. At stage I of the growth process, spherulites were too small, as shown in Fig. 12(a), to have effective interactions through polymer chains between the spherulites. Correspondingly, storage modulus of the composite sample did not change much. The duration of this stage was greatly influenced by the rate of nucleation which was affected by the OMMT and the PEOc contents. With the growth of spherulites, they began to have effective interactions with each other through entangled polymer network between them or even have direct contact with each other as shown in Fig. 12(b). At stage II of the growth process, G' of matrix sample began to increase and the growth rate became faster. The entanglement effect of PEOc greatly influenced the rheological response of matrix sample (G' and its increasing rate). At stage III, spherulites impinged into each other and space became crowded as shown in Fig. 12(c). The diminished interface area between spherulites and amorphous phases together with OMMT layers and the

entanglement of PEOc chains might hinder the mobility of iPP chains and slow down the transport of iPP chains into the crystalline region from the amorphous phases. So the growth rate of G' was slowed down slightly at this stage. After the crystallization was complete, POM samples were quickly quenched to room temperature. During the shrinkage and cooling process, the amorphous phases surrounding the spherulites were stretched because of the shrinkage of spherulites. Then some amorphous intercrystalline links were formed between the spherulites as indicated in Fig. 12(d) and (e).

4. Conclusion

In this study isothermal crystallization of iPP/OMMT and iPP/OMMT/PEOc composites was investigated by POM and rheometry. At the early stage of crystallization, OMMT layers played a dominant role in promoting the nucleation while PEOc played a role of inhibitor at this stage. However, PEOc caused another effect of concentration fluctuation assisted crystallization in the iPP/OMMT/PEOc ternary composites. With the growth of the spherulites, storage modulus of bulk material was increased. PEOc component greatly affected the increase of G' when proceeding into stage II of crystal growth process, such as the G' vs. t curve of PPCN5OE25 as shown in Fig. 5. At stage III of crystal growth process, the increase rate of G' was slowing down. This was because OMMT layers and the entanglement of PEOc chains limited the motion of polypropylene chains. Finally, during the shrinkage and cooling process after crystallization there formed some amorphous links between the spherulites, consisting of both PEOc and iPP chains.

Acknowledgements

The authors thank Dr. Ke Wang and Professor Qiang Fu of Sichuan University for their help to prepare the primary-batch of the sample, and also thank the generous financial support by following grants: National Natural Sciences Foundation of China, Grant Nos. 20574081 and 50773087, and the National Basic Research Program (973 program) No. 2003CB615600 of MOST.

References

[1] Ray SS, Okamoto M. Prog Polym Sci 2003;28:1539.
[2] Kawasumi M, Hasegawa N, Kato M, Usuki A, Okada A. Macromolecules 1997;30:6333.
[3] Giannelis EP. Adv Mater 1996;8:29.
[4] Gianelli W, Ferrara G, Camino G, Pellegatti G, Rosenthal J, Trombini RC. Polymer 2005;46:7037.
[5] Mishra JK, Hwang KJ, Ha CS. Polymer 2005;46:1995.
[6] Hwang JJ, Liu HJ. Macromolecules 2002;35:7314.
[7] Nascimento GM, Constantino VRL, Temperini MLA. Macromolecules 2002;35:7535.
[8] Bharadwaj RK. Macromolecules 2001;34:9189.
[9] Varga J. J Mater Sci 1992;27:2557.
[10] Li HH, Jiang SD, Wang JJ, Wang DJ, Yan SK. Macromolecules 2003;36:2802.
[11] Meille SV, Bruckner S, Porzio W. Macromolecules 1990;23:4114.
[12] Lotz B, Graff S, Straupe C, Wittmann JC. Polymer 1991;32:2902.
[13] Hoffman JD, Miller RL, Marand H, Roitman DB. Macromolecules 1992;25:2221.
[14] Somani RH, Yang L, Zhu L, Hsiao BS. Polymer 2005;46:8587.
[15] Li LB, de Jeu WH. Phys Rev Lett 2004;92:0775506-1.
[16] (a) Kumaraswamy G, Issaian AM, Kornfield JA. Macromolecules 1999;32:7537; (b) Kumaraswamy G, Verma RK, Issaian AM, Wang P, Kornfield JA, Yeh F, et al. Polymer 2000;41:8931; (c) Kumaraswamy G, Kornfield JA, Yeh F, Hsiao BS. Macromolecules 2002;35:1762.
[17] Lin YG, Mallin DT, Chien JCW, Winter HH. Macromolecules 1991;24:850.
[18] Pogodina NV, Winter HH. Macromolecules 1998;31:8164.
[19] Pogodina NV, Winter HH, Srinivas S. J Polym Sci Part B Polym Phys 1999;37:3512.
[20] Elmoumni A, Winter HH, Waddon AJ, Fruitwala H. Macromolecules 2003;36:6453.
[21] Elmoumni A, Winter HH. Rheol Acta 2006;45:793.
[22] Boutahar K, Carrot C, Guillet J. J Appl Polym Sci 1996;60:103.
[23] Boutahar K, Carrot C, Guillet J. Macromolecules 1998;31:1921.
[24] Devaux N, Monasse B, Haudin JM, Moldenaers P, Vermant J. Rheol Acta 2004;43:210.
[25] Zhang CG, Hu HQ, Wang DJ, Yan SK, Han CC. Polymer 2005;46:8157.
[26] Zhang CG, Hu HQ, Wang XH, Yao YH, Dong X, Wang DJ, et al. Polymer 2007;48:1105.
[27] Huo H, Jiang SC, An LJ. Polymer 2005;46:11112.
[28] Nam JY, Ray SS, Okamoto M. Macromolecules 2003;36:7126.
[29] Fornes TD, Paul DR. Polymer 2003;44:3945.
[30] Nowacki R, Monasse B, Piorkowska E, Galeski A, Haudin JM. Polymer 2004;45:4877.
[31] Ma JS, Zhang SM, Qi ZN, Li G, Hu YL. J Appl Polym Sci 2002;83:1978.
[32] Maio ED, Iannace S, Sorrentino L, Nicolais L. Polymer 2004;45:8893.
[33] Homminga DS, Goderis B, Mathot VBF, Groeninckx G. Polymer 2006;47:1630.
[34] Maiti M, Bandyopadhyay A, Bhowmick AK. J Appl Polym Sci 2006;99:1645.
[35] Tjong SC, Bao SP, Liang GD. J Polym Sci Part B Polym Phys 2005;43:3112.
[36] Wang X, Pang SL, Yang JH, Yang F. Trans Nonferrous Met Soc China 2006;16:s524.
[37] Lim JW, Hassan A, Rahmat AR, Wahit MU. J Appl Polym Sci 2006;99:3441.
[38] Ma XY, Liang GZ, Lu HJ, Liu HL, Huang Y. J Appl Polym Sci 2005;97:1907.
[39] Yang H, Zhang XQ, Qu C, Li B, Zhang LJ, Zhang Q, et al. Polymer 2007;48:860.
[40] Wang K, Wang C, Li J, Su JX, Zhang Q, Du RN, et al. Polymer 2007;48:2144.
[41] Sun TC, Dong X, Du K, Wang K, Fu Q, Han CC. Polymer 2008;49:588.
[42] Jafari SH, Gupta AK. J Appl Polym Sci 2000;78:962.
[43] Ishikawa M, Sugimoto M, Inoune T. J Appl Polym Sci 1996;62:1495.
[44] Zebarjad SM, Bagheri R, Seyed Reihani SM, Lazzeri A. J Appl Polym Sci 2003;90:3767.
[45] McNally T, McShane P, Nally GM, Murphy WR, Cook M, Miller A. Polymer 2002;43:3785.
[46] Pang YY, Dong X, Zhao Y, Han CC, Wang DJ. Polymer 2007;48:6395.
[47] (a) Inaba N, Sato K, Suzuki S, Hashimoto T. Macromolecules 1986;19:1690; (b) Inaba N, Yamada T, Suzuki S, Hashimoto T. Macromolecules 1988;21:407.
[48] Tanaka H, Nishi T. Phys Rev Lett 1985;55:1102.
[49] Tanaka H, Nishi T. Phys Rev A 1985;39:783.
[50] Wang H, Shimizu K, Kim H, Hobbie EK, Wang ZG, Han CC. J Chem Phys 2002;116:7311.
[51] Matsuba G, Shimizu K, Wang H, Wang ZG, Han CC. Polymer 2003;44:7459.
[52] Matsuba G, Shimizu K, Wang H, Wang ZG, Han CC. Polymer 2004;45:5137.
[53] Shimizu K, Wang H, Wang ZG, Matsuba G, Kim H, Han CC. Polymer 2004;45:7061.
[54] Zhang XH, Wang ZG, Muthukumar M, Han CC. Macromol Rapid Commun 2005;26:1285.
[55] Zhang XH, Wang ZG, Dong X, Wang DJ, Han CC. J Chem Phys 2006;125:024907.
[56] Meng K, Dong X, Zhang XH, Zhang CG, Han CC. Macromol Rapid Commun 2006;27:1677.
[57] Yao YH. Ph.D. thesis, Institute of Chemistry, Chinese Academy of Sciences; 2006.
[58] Keith HD, Padden FJ, Vadimsky RG. J Polym Sci Part A2 1966;4:267.
[59] Keith HD, Padden FJ, Vadimsky RG. J Appl Phys 1966;37:4027.
[60] Keith HD, Padden FJ, Vadimsky RG. J Appl Phys 1971;42:4585.
[61] Keith HD, Padden FJ, Vadimsky RG. J Polym Sci Polym Phys Ed 1980;18:2307.